Research Article **Open Access**

Shivanand Mali* Baleshwar Singh

3D Numerical Modeling of Large Piled-Raft Foundation on Clayey Soils for Different Loadings and Pile-Raft Configurations

https://doi.org/10.2478/sgem-2019-0026
received December 3, 2018; accepted August 21, 2019.

Abstract: In a piled-raft foundation, the interaction between structural elements and soil continuum can be simulated very precisely by numerical modeling. In the present study, 3D finite element model has been used to examine the settlement, load-sharing, bending moment, and shear force behavior of piled-raft foundation on different soil profiles for different load configurations and pile-raft configurations (PRCs). The model incorporates the pile-to-soil and raft-to-soil interactions by means of interface elements. The effect of parameters such as pile spacing and raft thickness are also studied. For any soil profile, larger pile spacing is observed to be more efficient in reducing the average settlement and enhancing the load-sharing coefficient. The smaller pile spacing is observed to be efficient in reducing the differential settlement. For any soil profile, the behavior of piled-raft foundation is significantly affected by the PRCs and load configurations. Furthermore, the raft thickness has significant effect on settlement, bending moment, and shears force. Thus, the results of the present study can be used as guidelines for analyzing and designing large piled-raft foundation.

Keywords: Piled raft, Numerical modeling, Clay soil, Load configurations, Pile-raft configurations.

1 Introduction

Piled raft is a geotechnical foundation consisting of three elements raft, piles, and soil domain. The piles can be used to reduce the settlement of the raft foundation (Burland 1977). Also, several studies suggested that the piles in piled raft can be used to carry some part of the superstructure load. The distribution of among load among the piles, raft, and soil depends on their relative stiffness. On the basis of the dimensions of the raft and piles, the piled raft can be classified as a small piled raft ($B_r < L_p$) and large piled raft ($B_r > L_p$) (Viggiani 2001). In a small piled raft, the primary reason to add the piles is to achieve a sufficient factor of safety against the bearing failure. However, in a large piled raft, piles are added essentially to reduce the settlement.

The centrifuge tests had been carried to understand the settlement behavior of piled rafts with different pile arrangements (Nguyen et al. 2013). They showed that the piled raft model with a concentrated pile arrangement (piles of uniform length concentrated at center of raft) can effectively decrease the total and differential settlements in comparison with the pile raft model with a uniform pile arrangement (piles spread over the entire area of raft). The behavior of large piled-raft foundation on clay soil is studied by numerical modeling (Mali & Singh 2018 & 2019). The results indicated that with the 5 to 6 times increase in the pile diameter of pile spacing , both the average settlement ratio and the differential settlement ratio decreased effectively, and thereafter, it increased gradually. Raft with smaller raft-to-soil stiffness ratio and larger pile group-to-raft width ratio observed to be effective in decreasing the average settlement ratio.

An undrained behavior of a piled raft system was assessed by average and differential settlements, raft bending moment, and pile butt load ratio (Ghalesari et al. 2015). They showed that a piled raft with variable pile length (length of center pile is more than the outer pile) and optimal arrangement yields the most economical

***Corresponding author: Shivanand Mali,** Research Scholar, Department of Civil Engineering, Indian Institute of Technology Guwahati, Guwahati-781039, Assam, India, E-mail: shivanandmali2016@gmail.com
Baleshwar Singh, Department of Civil Engineering, Indian Institute of Technology Guwahati, Guwahati-781039, Assam, India

and practical design. Similarly, the piled rafts subjected to concentrated loading showed lower differential settlements and higher pile loads than those of uniform loading (Ghalesari et al. 2016).

Furthermore, some studies indicated that the piled raft can be used as an effective and economic foundation alternative for tall buildings to control the settlement and to enhance the bearing capacities (Poulos and Devdas 2005; Poulos and Bunce 2008; Poulos et al. 2011; Rabiei and Choobbasti 2016). Several researchers have investigated the settlement (Prakoso and Kulhawy 2001; Chow et al 2012) and bearing behavior (Reul 2004; Reul and Randolph 2004; Sanctis and Mandolini 2006; Lee et al. 2010) of a piled-raft foundation on clay soils under uniformly distributed loading. The finite layer method was used to investigate the behavior of piled rafts with piles of different lengths and diameters under vertical loading (Chow and Small 2005). They reported that for non-uniform loading, the use of long piles underneath the heavily loaded area can help to minimize the risk of tilting as well as to reduce the overall and differential settlements.

The concentrated or point loading is commonly encountered in the practice. As discussed earlier, most of the studies have modeled the piled rafts under uniform distributed loading with a uniform pile length. However, very few studies included the effect of load configurations, pile-raft configurations (PRCs), and other geometrical parameters on the behavior of large piled-raft foundation. Thus, further investigation is required to understand the behavior of large piled-raft foundation for different load configurations and PRCs. The objective of the present study is to understand the effects of load configurations, PRCs, pile spacing, and raft thickness on settlement, load-sharing, bending, and shear behavior of piled-raft foundation on soft clay and stiff clay soil profiles. The different configurations used in the study are discussed in Section 3. An analysis of the piled raft has been performed using PLAXIS 3D software (Brinkgreve et al. 2015). A series of numerical simulations for different PRCs was performed to fulfill the aim of the present study.

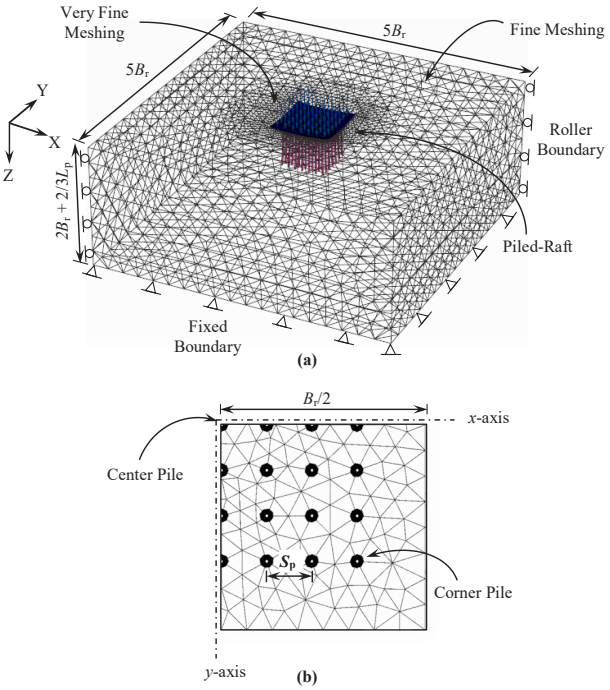

Figure 1: (a) Typical finite element mesh used in the parametric study. **(b)** Plan view (quarter of the piled raft)

2 Finite Element Modeling

2.1 Finite Element Mesh and Boundary Conditions

The model consists of the soil continuum with unaffected boundary conditions, foundation geometry with square raft of 45 m width (B_r), interface element and the applied uniformly distributed load (*UDL*) of 150 kPa, or equivalent point loading (*EPL*). Figure 1 shows the typical finite element mesh used in the present study. The water table was assumed at ground level. As the water table was assumed at ground level, the undrained analysis is used in the present study. Also, the undrained analysis is often much easier to carry out, inexpensive to get the design parameters, and is necessary to assess the short-term stability that can be more critical than the long-term stability. From the edge of the raft, lateral soil domain boundaries of the model were placed at a distance of twice the width of raft and restrained against horizontal translation (i.e., horizontal displacement) but with vertical translation (i.e., vertical displacement) of soil being allowed.

The pressure bulb in a raft foundation was formed up to twice the width of raft, while that in pile group was formed at two-third of the pile length. Thus, the bottom soil boundary was at a vertical distance of twice the width of raft plus two-third of the pile length and was restricted from both horizontal and vertical translations. Globally, fine mesh has been selected for the entire soil domain, and relatively, very fine mesh was chosen in the vicinity of the structural elements. The very fine meshing has been generated with coarseness factor of 0.25, that is, the size

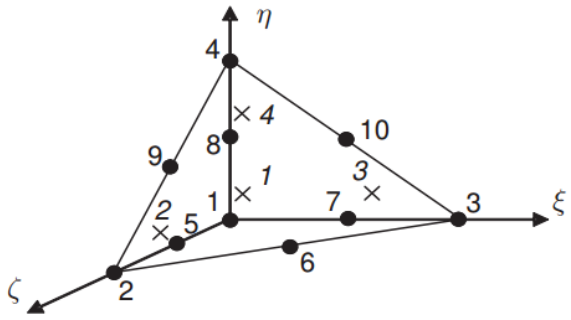

Figure 2: A 10-node tetrahedral element (Brinkgreve et al. 2015)

of element in very fine meshing is 0.25 times that of size of element in fine meshing.

The analysis of piled raft involved two stages, namely, initial stage and loading stage. In the initial stage (i.e., initial geometry configurations and corresponding initial stress field), the soil domain was activated, and in the loading stage, the piled-raft geometry and applied load were activated and run was made. From the preliminary analysis of the unpiled raft under the applied loading, the selected lateral boundaries of the soil domain were sufficient because the observed zone of plastic strain developed in the soil was equal to width of raft (B_r) laterally from the edge of the raft.

2.2 Constitutive Modeling

The Mohr–Coulomb model requires lesser number of input parameter than other models. The soil was modeled as 10-node tetrahedral elements with the elastic-perfectly plastic Mohr–Coulomb model (Fig. 2). The parameters required for modeling consisted of cohesion, angle of internal friction, Young's modulus, and Poisson's ratio. As per the Mohr–Coulomb failure criteria, the yielding or failure takes place in the soil mass as the mobilized shear stress at any plane becomes equal to the shear strength of soil.

To simplify the analysis process, the constant values of the material parameters were used for the entire soil domain. A short description of soil constitutive model has been given in Appendix. The raft was modeled as 5-node triangular plate elements. After meshing, plates are composed of 6-node triangular plate elements with six degrees of freedom per node (three translational and three rotational). The plate elements are based on Mindlin's plate theory. This theory allows for plate deflection because of shearing as well as bending. In addition, the element can change length when an axial force is applied. Plate elements can become plastic if a prescribed maximum bending moment or maximum axial force is reached.

The piles were modeled as 4-node embedded beam elements. An embedded beam consists of beam elements with special interface elements providing the interaction between the beam and the surrounding soil. The piles are basically considered as bored piles. After meshing, the beam elements are 3-node line elements with six degrees of freedom per node (three translational and three rotational). Element stiffness matrices are numerically integrated from the four Gaussian integration points (stress points). The element allows for beam deflections because of shearing as well as bending. In addition, the element can change length when an axial force is applied.

The raft and piles remains in elastic state as their modulus of elasticity is greater than the soil; therefore, the material of raft and piles was considered to be linear elastically. The piles and raft were connected by rigid connection. In this analysis, the interface element is modeled by interface reduction factor (R_{inter}). R_{inter} indicates the strength of interface element as a percentage of the shear strength of adjacent soil. Interface elements follow the Mohr–Coulomb failure criterion; once the shear stress in soil equal to the yield shear strength of the soil, the slippage occurs at the interface.

The raft–soil interface was considered as a smooth contact with an R_{inter} of 0.67. The interaction between the soil and the pile was modeled by the embedded interface elements of 3-node line elements with pairs of nodes instead of single nodes. One node of each pair belongs to the beam element, whereas other node is point in the 10-node wedge element belonging to soil element. After meshing, interfaces are composed of 12-node interface elements. In the finite element formulation, the coordinates of each node pair are identical, which indicates that the interface element has a zero thickness. Interface elements were introduced mainly to simulate the displacement discontinuity between the structural elements (raft and piles) and the soil mass.

2.3 Model Validation

The present finite element model in the PLAXIS 3D has been validated by comparing with the reported results of Sinha and Hanna 2016. A raft of 24 m × 24 m size with a 2-m thickness and 16 piles of 1-m diameter with different lengths (5, 10, and 15 m) were used in the study. The piles were spaced at six times of pile diameter, and uniformly a distributed load of 0.5 MPa was applied on the foundation. The material properties of the soil, raft, and piles are given in Table 1. The comparative results of the present study with the reported results are shown in

Table 1: Material properties used in the validation (Sinha and Hanna 2016)

Material	Properties	Unit	Value
Soil	Young's modulus, E_s	MPa	54
	Poisson's ratio, v_s	-	0.15
	Unit weight, γ	kPa	19
	Angle of internal friction, φ	°	20
Raft	Young's modulus, E_r	GPa	34
Pile	Young's modulus, E_p	GPa	25
	Poisson's ratio, v_p	-	0.2

Table 2: Material properties used in the parametric analysis

Material	Properties	Unit	Value
Soil	Unsaturated unit weight, γ_{unsat}	kN/m^3	16
	Young's modulus, E_s	MPa	25 (Soft clay) 82 (Stiff clay)
	Poisson's ratio, v_s	-	0.495
	Angle of internal friction, φ	°	0
	Undrained cohesion	kPa	25 (Soft clay) 80 (Stiff clay)
Raft	Young's modulus, E_r	GPa	25
	Poisson's ratio, v_r	-	0.25
Pile	Young's modulus, E_p	GPa	25
	Poisson's ratio, v_p	-	0.25

Table 3: Geometric configurations of pile-raft model for parametric analysis

Parameters	Unit	Value
Raft width, B_r	m	45
Raft width, L_r	m	45
Raft thickness, t_r	m	0.5, 1, 1.5, 2*
Number of piles	-	49
Pile length, L_p	m	30*
Pile spacing, S_p	m	3*, 4, 5, 6, 7
Width of pile group, B_g (Corresponding to each S_p)	m	19, 25, 31, 37, 43
Pile diameter, d_p	m	1

* Indicates standard value if not varied.

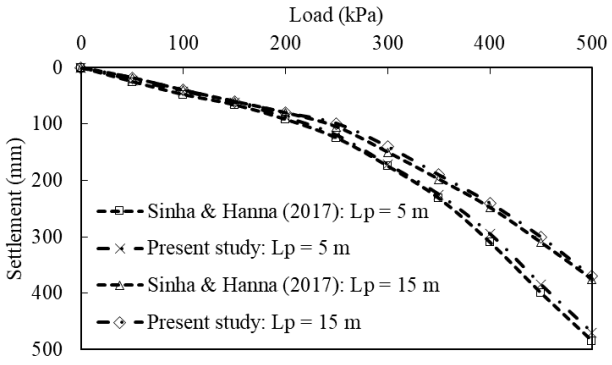

Figure 3: Comparison of load settlement behavior of the present study with the results of Sinha and Hanna (2016)

Figure 3. It can be seen that the results of the present study are in reasonably good agreement with those reported for the different lengths of piles. For continuing the accuracy of the results, similar modeling steps have been followed to model the different PRCs of the present study.

2.4 Parametric Study

In the parametric study, the settlement, load-sharing, bending moment, and shear force behavior of the large piled-raft foundation on different soil profiles were studied for different load configurations and PRCs. These behaviors were investigated by varying pile spacing (S_p) and raft thickness (t_r). The properties of soil, raft, and piles are summarized in Table 2. The soft clay soil profile having c_u = 25 kPa and E_s = 25 MPa and stiff clay soil profile having c_u = 80 kPa with E_s = 82 MPa were selected (Ranjan and Rao 2007).

In all the parametric study, only one parameter was varied at a time and standard values were selected for all other parameters (Table 3). The geometrical dimensions of piled raft and the values of E_r and E_p were selected from Viggiani 2001. Figure 4 shows the plan view of column locations and PRCs. The width of pile group (B_g) corresponding to the pile spacings of 3, 4, 5, 6, and 7 m were 19, 25, 31, 37, and 43 m. A total of 49 columns were arranged in square pattern and were spaced (S_c) at 6-m distance (center to center) from each other (Fig. 4a).

For different pile spacings (3–7 m), in all PRCs, a total of 49 piles had been arranged (7 rows × 7 column), with minimum 1-m clear distance from the raft edge to the pile outer edge. The load configurations (LC) and PRCs) are depicted in Figure 5. Load configuration consisted of uniformly distributed load, *UDL* (LC1), and equivalent point loads *EPL* (LC2) (Fig. 5a). The *UDL* of 150

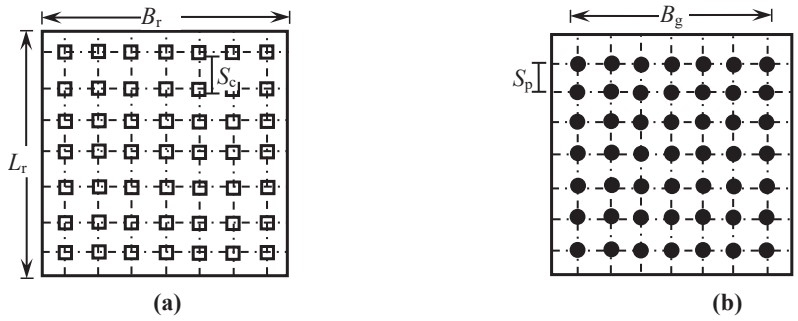

Figure 4: (a) Location of column and **(b)** top view of pile-raft configurations

kPa was applied on the foundation, and corresponding magnitudes of the point loading *EPL* was also considered. For application of *EPL*, the *UDL* was distributed into 49 points (magnitude of each 6,199 kN) and their line of application passes through the center of the columns. The different PRCs such as PRC with uniform pile length, PRC with "W"-shaped non-uniform pile length, and PRC with "V"-shaped non-uniform pile length were used in this study (Fig. 5b).

The PRCs were altered in such way that the total length of piles L_t in each PRC became 1,470 m. In all the PRCs, piles of equal length were provided in each square loop (SL) as shown in the plan view of raft (Fig. 5b). Also, the length of center pile (P_1) was different in each PRC. However, in PRC1(a) or PRC2(a), piles of uniform length were provided (L_p = 30 m). As far as the practical application of such PRC is concerned, in the foundation of Messe Turm Tower (Frankfurt), raft of non-uniform thickness and non-uniform pile length (length was more at center and decreasing towards the edges of raft) had been used successfully (Poulos 2001). The PRC with "W"-shaped non-uniform pile length had been analyzed to understand its performance over the other configurations.

The average settlement (W_{avg}) of piled-raft is calculated using Eqn. (1), as proposed by Reul and Randolph 2004. The differential settlement (W_{diff}) of piled-raft is calculated using Eqn. (2). The vertical settlement at the center (w_{center}) and corner (w_{corner}) of the raft were used directly to calculate W_{avg} and W_{diff} of the piled raft.

$$W_{\text{avg}} = \frac{1}{3}(2w_{\text{center}} + w_{\text{corner}}) \quad (1)$$

$$W_{\text{diff}} = (w_{\text{center}} - w_{\text{corner}}) \quad (2)$$

where w_{center} is the center settlement of raft and w_{corner} is the corner settlement of raft. The load-sharing ratio (α_{pr}) is defined as the ratio of total load carried by the piles (R_{pile}) to the applied load (R_{total}) on the foundation (Eqn. (3)). R_{pile} is calculated by summing the axial load carried by the individual piles at its head. The value of α_{pr} = 1 represents the freestanding pile group, whereas α_{pr} = 0 indicates the unpiled raft. In case of piled raft, the value of α_{pr} lies between 0 and 1.

$$\alpha_{pr} = \frac{R_{pile}}{R_{total}} \quad (3)$$

Table 4 summarizes the lengths of piles and number of piles used for different PRCs. Several trials have been conducted to select the lengths of piles for different PRCs. The abbreviation L_{1W} and L_{1V} indicates the length of pile number "one" (P_1) in "W"-shaped and "V"-shaped PRCs, respectively.

3 Results and Discussion

This section discusses the effect of pile spacing (S_p), raft thickness (t_r), load configuration (LC), and PRC on average settlement (W_{avg}), differential settlement (W_{diff}), load-sharing ratio (α_{pr}), maximum bending moment (M_{max}), and maximum shear force (τ_{max}). The pile spacing and raft thickness have significant effect on the behavior of piled-raft foundation. Therefore, the effect pile spacing and raft thickness on different PRCs has been studied and are presented in the respective sections.

3.1 Effect of Pile Spacing

3.1.1 Effect of Pile Spacing on Settlement

In order to understand the effect of pile spacing, S_p has been varied from 3 to 7 m, whereas for other parameters such as raft size (B_r), raft thickness (t_r), and pile diameter

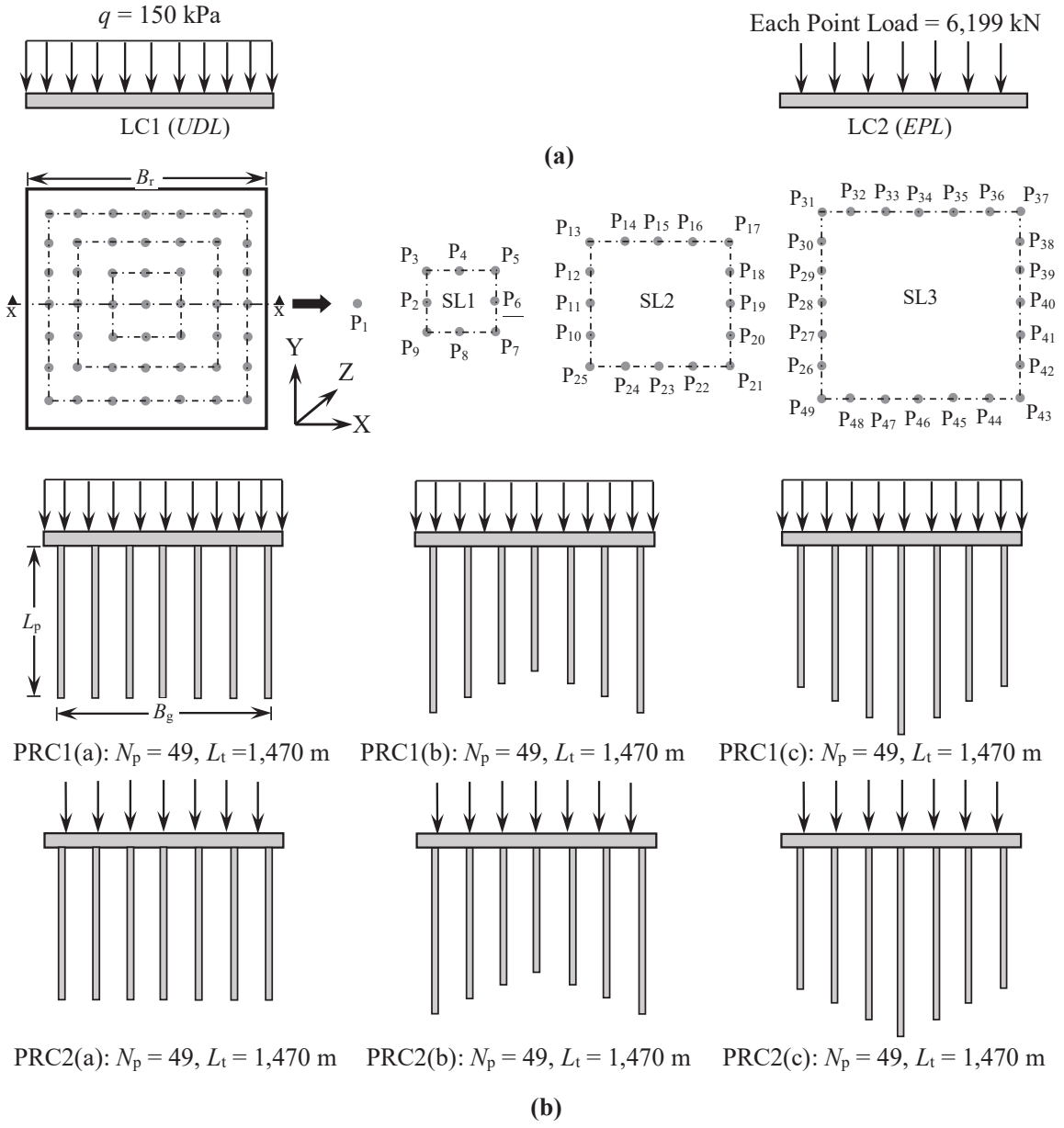

Figure 5: Different configurations used in the parametric study: (a) load configurations (LCs) and (b) pile-raft configurations (PRCs)

Table 4: Pile lengths used for different pile-raft configurations

Name and no. of piles, N_p	Pile length, L_p (m)		
	PRC with uniform pile lengths	PRC with "W"-shaped pile lengths	PRC with "V"-shaped pile lengths
P_1 (1 pile)	30	L_{1W} = 24.46	L_{1V} = 37.19
P_2–P_9 (8 piles)		$L_{2\text{-}9W} = 1.1\ L_{1W}$ = 26.91	$L_{2\text{-}9V} = L_{1V}/1.1$ = 33.81
P_{10}–P_{25} (16 piles)		$L_{10\text{-}25W} = 1.1\ L_{2\text{-}9W}$ = 29.60	$L_{10\text{-}25V} = L_{2\text{-}9V}/1.1$ =30.74
P_{26}–P_{49} (24 piles)		$L_{26\text{-}49W} = 1.1\ L_{10\text{-}25W}$ = 32.56	$L_{26\text{-}49V} = L_{10\text{-}25V}/1.1$ =27.94

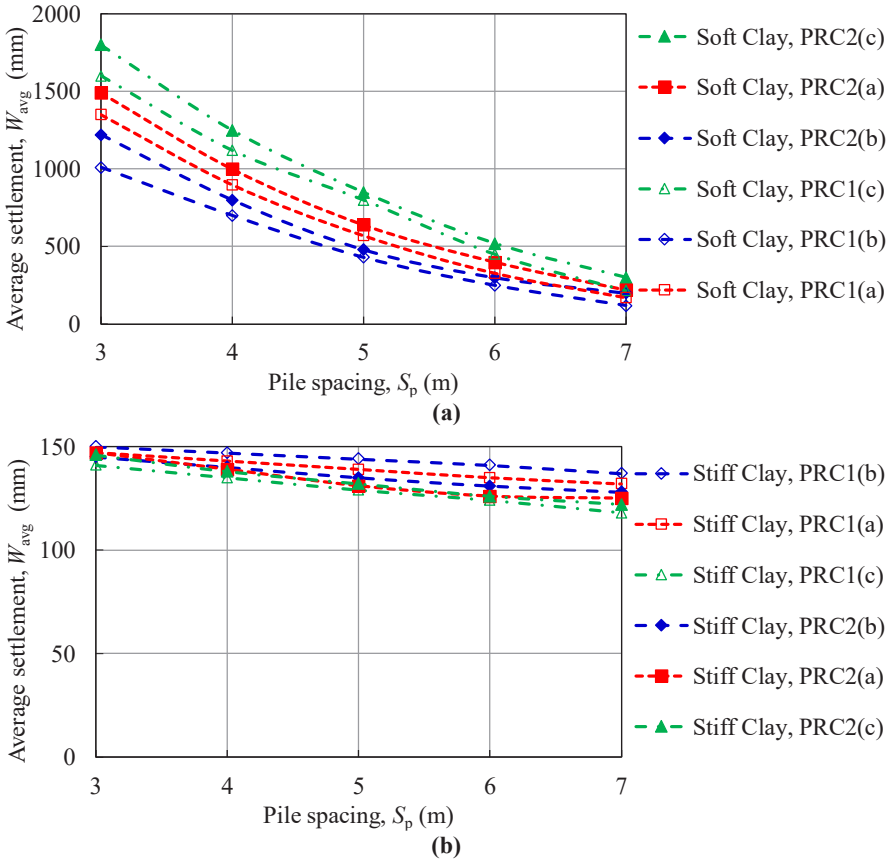

Figure 6: Effect of pile spacing on the average settlement for different pile-raft configurations: (a) soft clay and (b) stiff clay

(d_p), standard value has been chosen from Table. 3. As mentioned earlier, all the PRCs used in the present study consist of an applied load of 150 kPa and a total pile length of 1,470 m. The effect of S_p on W_{avg} for different PRCs and for different types of soil (soft clay and stiff clay) is shown in Figure 6(a) and 6(b), respectively.

It can be seen that for any PRC with any soil profile (soft clay or stiff clay), W_{avg} decreases as the S_p increases. However, the rate of decrease in W_{avg} is observed to be substantial in case of soft clay soil profile as compared to that of the stiff clay soil profile. Here, it should be noted that with an increase in the pile spacing (with constant number of piles), width of pile group B_g increases, which results in the increase in the area covered by the piles (A_g). As the area covered by the piles increases (A_g), piles get uniformly distributed under the entire area of the raft (A_r) and because of which the average settlement of the pile-raft decreases. In stiff clay, soil is relatively stiff than that of soft clay soil; thus, the rate of decrease in W_{avg} is minimum in stiff clay soil.

For any soil profile, W_{avg} is observed to be lower for PRC with *UDL* when compared to the PRC with *EPL*. Moreover, for soft clay soil profile, the difference in W_{avg} is significant at lower pile spacing than that at larger pile spacing. For example, at the 3-m pile spacing, the W_{avg} of PRC1(b) was 1,010 mm and of PRC2(b) was 1,220 mm. While at the 7-m pile spacing, the W_{avg} of PRC1(b) was 120 mm and of PRC2(b) was 180 mm.

At lower pile spacing (S_p = 3 m), piles were mainly concentrated near the center portion (B_g = 19 m) of the raft; however, the applied load (*UDL* or *EPL*) was acting over the entire raft. Because of which, at lower pile spacing, the difference in W_{avg} was significant than that of larger pile spacing (S_p = 7 m). Thus, for better prediction of average settlement, the actual loading encountered in the practice (i.e., point or concentrating load, *UDL*, and line load) should be simulated in the modeling of piled-raft foundation.

For pile-raft foundation rested on soft clay soil and stiff soil profile, PRC(b) or "W"-shaped PRC and PRC(c) or "V"-shaped PRC with larger pile spacing can be used effectively to reduce the W_{avg}, correspondingly (Fig. 6a and b). Thus, it can be concluded that the effectiveness of PRC depends on the condition of soil (soft or stiff)

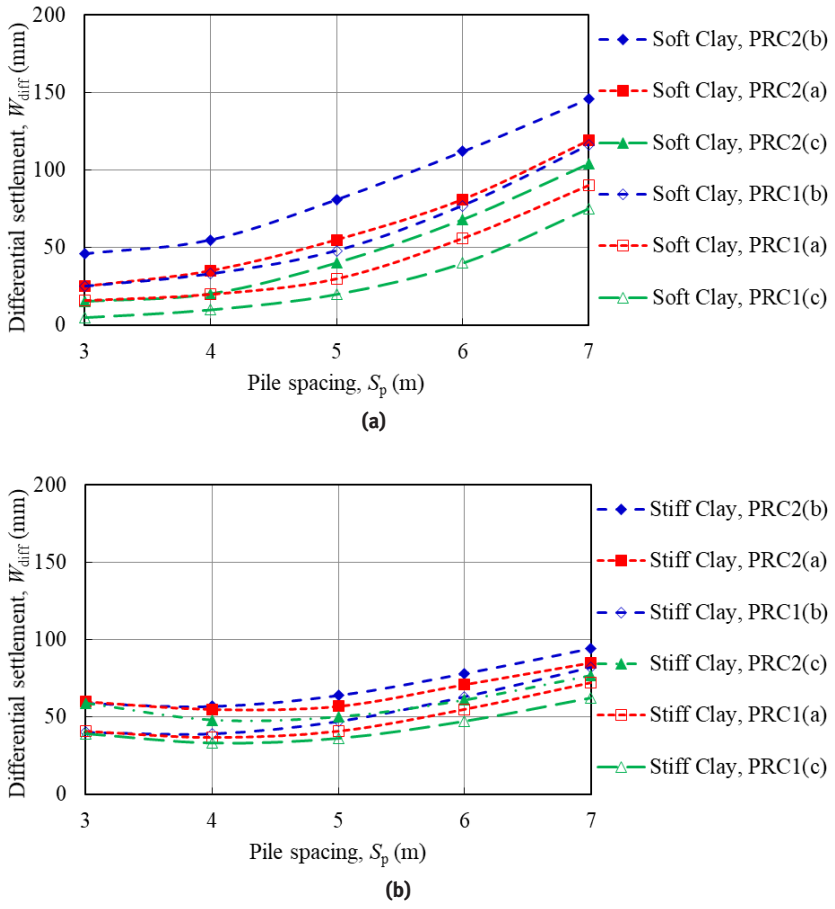

Figure 7: Effect of pile spacing on differential settlement for different pile-raft configurations: **(a)** soft clay and **(b)** stiff clay

beneath the raft. Moreover, as per the codal requirement, the allowable maximum settlement of the raft foundation is 125 mm and the allowable differential settlement is 148.5 mm (0.0033*Br) (IS 1904-1986). Therefore, pile spacing should be selected in such way that the values of maximum settlement and differential settlement are within allowable limits.

As the pile spacing increases, the trends observed for differential settlement are opposite to that of average settlement trends. For any PRC with any soil profile, W_{diff} increases as the S_p increases (Fig. 7). In case of soft clay soil profile, the rate of increase in W_{diff} is more significant than that of stiff clay soil profile. As stated earlier, with the increase in S_p, piles get spread away from the center of the raft, which results in the increase in pile group area A_g and subsequent decrease in the center settlement W_{center} of the raft (because piles start behaving as individual element). However, the difference between center and corner settlement increases.

Moreover, for soft clay soil profile at larger pile spacing, the relative difference in W_{diff} is significant as that of stiff clay soil profile (Table 5). Alike W_{avg}, for any PRC with any soil profile, W_{diff} is observed to be lower for PRC with *UDL* as compared to the PRC with *EPL*. For example, at the 3-m pile spacing for soft clay soil profile, the W_{avg} of PRC1(b) is 25 mm, whereas for PRC2(b), it is 46 mm.

For any load configuration and any soil profile, PRC(c) or "V"-shaped PRC with lower S_p can be used effectively to reduce the W_{diff} (Fig. 7b). In PRC(c) or "V"-shaped PRC, longer piles cover the center part of the raft because of which differential settlement decreases. Here, it should be noted that for any PRC, the total pile length is equal to 1,470 m. So, it is suggested to use the longer piles at the center part of the raft to reduce the differential settlement effectively rather than providing the uniform pile length under the raft.

3.1.2 Effect of Pile Spacing on Load-Sharing Ratio

Among the several other parameters, pile length and pile spacing are considerably affecting the load carried by the

Table 5: Center and corner settlement for different pile-raft configurations at different pile spacings

Pile-raft configurations	Pile spacing, S_p (m)	Settlement in soft clay soil profile (mm)			Settlement in stiff clay soil profile (mm)		
		W_{center}	W_{corner}	W_{diff}	W_{center}	W_{corner}	W_{diff}
PRC1(a)	3	490	474	16	160	147	41
PRC1(b)		916	891	25	157	117	40
PRC1(c)		1135	1125	10	158	119	39
PRC1(a)	7	211	121	90	144	72	72
PRC1(b)		232	116	116	150	68	82
PRC1(c)		243	162	81	139	77	62

piles in piled-raft foundation. The contribution of piles in piled raft needs to be estimated for economical and efficient design of piled-raft foundation. The effect of S_p on load-sharing coefficient (α_{pr}) for different piled-raft configurations and different soil profiles are shown in Figure 8.

For any PRC with any soil profile, α_{pr} increases linearly (approximately) as the S_p increases. Also, a lower value of α_{pr} is observed for the PRC with *UDL* than that of PRC with *EPL*. In case of point loading, the load is concentrated at single points, whereas in later case, the load is uniformly distributed over the entire area. Moreover, earlier studies have also reported that the load carried by piles for concentrated loading were generally greater than those of uniform loading (Ghalesari and Choobbasti 2016; Lee et al 2010). It can be also observed from Figure 8(a) that at larger pile spacing (S_p = 6-7 m), α_{pr} in soft clay soil profile is relatively higher than stiff soil profile.

Thus, for uniform distributed load, the contribution of pile bearing obtained was less than that of the point load. Furthermore, the calculated number of piles required to carry the applied load will be more for *UDL* than that of *EPL*. However, the addition of more number of piles may result into unnecessarily over safe design. Therefore, for efficient and economical design of foundation, attention should be given to simulate the loading condition as close as possible in the modeling.

It is interesting to note that for any load configuration with any soil profile, PRC(b) or "W"-shaped PRC observed to be more effective in enhancing the α_{pr}. In "W"-shaped PRC, piles in center part of the raft are relatively lesser in length compared to those of other PRCs. In "W"-shaped PRC, maximum pile capacities have been mobilized (higher soil confinement because of the W shape arrangement) because of the shorter length of piles at the center part of the raft. Table 6 presents the load carried by piles in different PRCs at different pile spacings.

3.1.3 Effect of Pile Spacing on Maximum Bending Moment

Normally, the raft foundation is designed for maximum bending moment and maximum shear force values. Thus in the present study, the maximum bending moment and maximum shear force values are taken into account. The effect of S_p on M_{max} for different PRCs and different soil profiles is presented in Figure 9. For any PRC with any soil profile, M_{max} is observed to increase with the increase in S_p. PRC with soft clay soil profile possesses lower M_{max} (Fig. 9a) as compared to stiff clay soil profile (Fig. 9b).

Also, for any PRC with any soil profile, M_{max} is observed to be lower for PRC with *UDL* as compared to the PRC with *EPL*. For example, at the 3-m pile spacing for soft clay soil profile, the M_{max} of PRC1(b) is 2,400 kN m, whereas for PRC2(b), it is 3,150 mm. For any load configuration and any soil profile, PRC(c) or "V"-shaped PRC was more effective in reducing the M_{max}.

3.1.4 Effect of Pile Spacing on Maximum Shear Force

The effect of S_p on τ_{max} for different PRCs and different soil profiles is presented in Figure 10. For any PRC with any soil profile, τ_{max} is observed to increase with the increase in S_p (except for PRC with S_p = 6 m and *EPL*). Because columns are located at 6-m spacing, the shear force decreases abruptly. PRC with soft clay soil profile possesses lower τ_{max} as compared to stiff clay soil profile (except S_p = 3 m). Also, for any PRC with any soil profile, τ_{max} is lower for

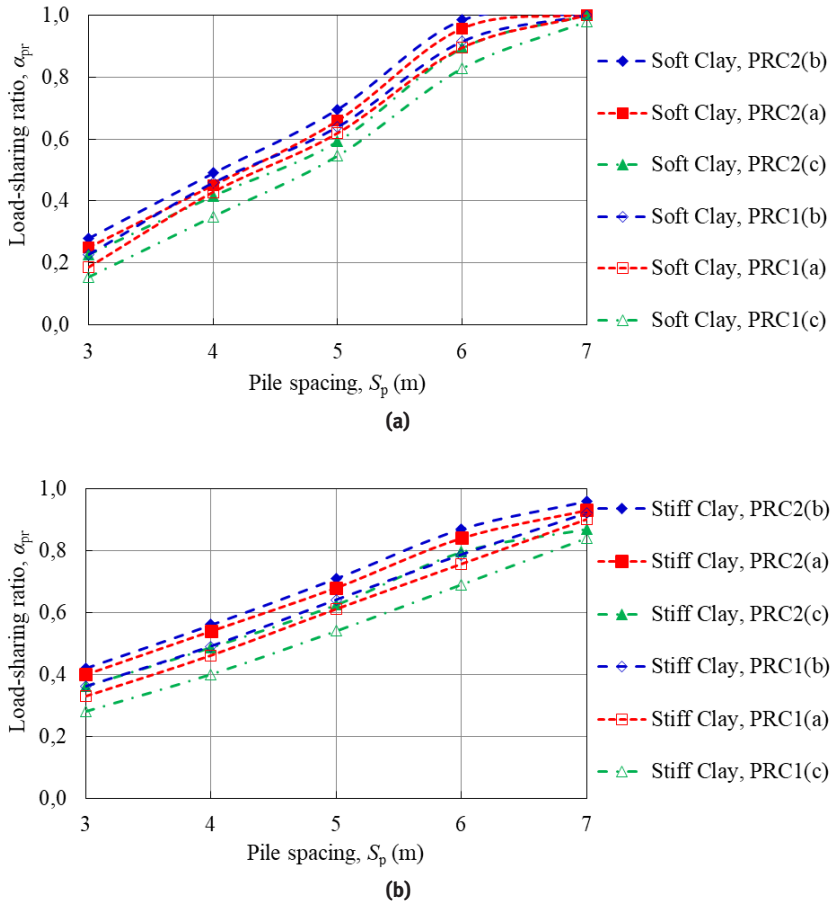

Figure 8: Effect of pile spacing on load-sharing coefficient for different pile-raft configurations **(a)** soft clay and **(b)** stiff clay

Table 6: Load carried by piles in different pile-raft configurations at different pile spacings

Pile-raft configurations	Pile spacing, S_p (m)	Soft clay: load-carried by piles, R_{pile} (kN)			Stiff clay: load-carried by piles, R_{pile} (kN)		
		R_{center}	R_{edge}	R_{corner}	R_{center}	R_{edge}	R_{corner}
PRC1(a)	3	226	2076	4434	565	3010	5854
PRC1(b)		431	3125	5597	650	3640	6723
PRC1(c)		494	1272	2765	1593	1474	3360
PRC1(a)	7	6721	7036	8579	6221	6388	5031
PRC1(b)		4890	7836	9105	4728	6879	5102
PRC1(c)		7376	6309	8240	7222	5751	4799

PRC with *UDL* (except at S_p = 6 m) as compared to the PRC with *EPL*.

For any load configuration and any soil profile, PRC(c) or "V"-shaped PRC is more effective in reducing the τ_{max}. Therefore, for lower bending and shear force in piled raft, it is suggested to use longer length of piles at the center of raft and relatively smaller piles towards the edge of the raft. The comprehensive study on design and applications of piled raft foundations has been reported in the literature (Poulos 2001). The study showed that the maximum settlement of piled raft was marginally affected by uniform and concentrated loading, whereas

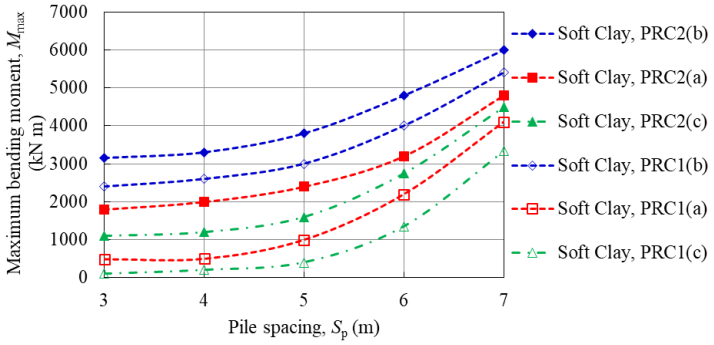

(a)

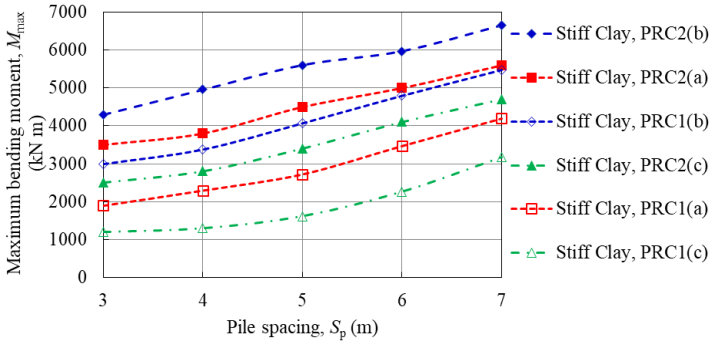

(b)

Figure 9: Effect of pile spacing on maximum bending moment for different pile-raft configurations **(a)** soft clay and **(b)** stiff clay

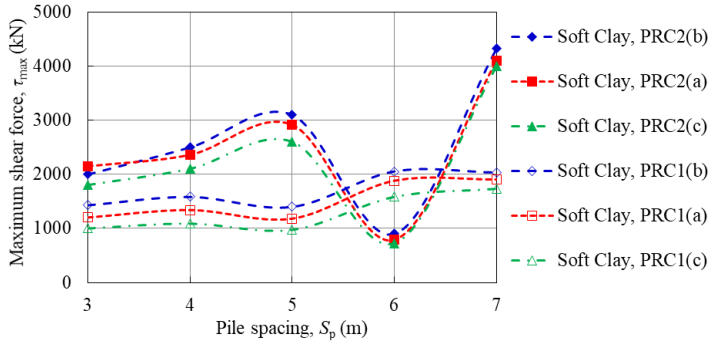

(a)

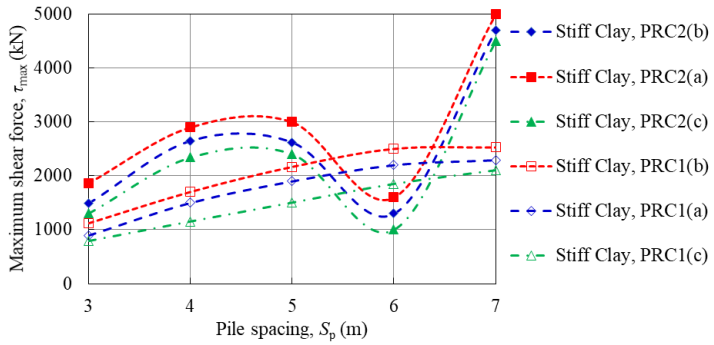

(b)

Figure 10: Effect of pile spacing on maximum shear force for different pile-raft configurations **(a)** soft clay and **(b)** stiff clay

the differential settlement and bending moment of raft were higher for concentrated loading (alike present study) and, the percentage loads carried by the piles were independent of the type of loading. The foundation design with minimum bending moment and minimum shear force may be more economical; therefore, in subsequent sections, PRC(c) or "V"-shaped PRC and more realistic loading LC2 or EPL has been selected and the effect of raft thickness is studied.

3.1.5 Effect of Raft Thickness on Settlement

The behavior of piled raft is dependent on the flexibility or stiffness of the raft. In order to assess the flexibility/stiffness of the raft, raft-to-soil stiffness ratio (Viggiani 2001) has been used in the present study and is presented in Eqn. (4).

$$K_{\mathrm{rs}} = \frac{4\times E_{\mathrm{r}}\times(1-\nu_s^2)}{3\times E_{\mathrm{S}}(1-\nu_r^2)} \times \frac{t_r^3}{B_r^3} \tag{4}$$

where E_r is the Young's modulus of raft; ν_s is the Poisson's ratio of soil; E_s is the elastic modulus of soil, ν_r is the Poisson's ratio of raft; B_r is the width of the raft, and t_r is the thickness of raft.

Thus, it can be observed from Eqn. 4 that with the increases in raft thickness, raft-to-soil stiffness ratio also increases. Moreover, the K_{rs} = 0.001 indicates the perfectly flexible, K_{rs} value I the range of 0.001–1 indicates intermediate flexibility, and $K_{rs} \geq 1$ indicates the perfectly stiff (Viggiani 2001). The calculated K_{rs} values for a raft thickness of 0.5, 1, 1.5, and 2 m are 0.0015, 0.0118, 0.0398, and 0.0943, respectively, for the present study. The raft with t_r = 0.5 m is comparatively more flexible than other raft thickness.

3.1.6 Effect of Raft Thickness on Settlement

The effect of t_r on W_{avg}, and W_{diff} for PRC2(c) and different soil profiles has been presented in Figure 11a and 11b, respectively. It is interesting to note that, with the increase in t_r, W_{avg} also increases. The increase in W_{avg} is due to the increase in self weight of the raft as the t_r increases. The optimum design from static response of pile–raft interaction had been discussed and developed by Ghalesari et al. (2015). They also reported that the increase in raft thickness may increase the average settlement of piled rafts under uniform load.

Furthermore, as expected the increase in W_{avg} is observed to be substantial in case of soft clay soil profile (Fig. 11a). Usually, soft clay soils are susceptible for larger settlement because it possesses low undrained shear strength. For any soil profile, W_{diff} decreases as the t_r increases. With the increase in raft thickness, raft becomes stiffer, and because of this, W_{diff} also decreases. Moreover, the decrease is observed to be significant in soft clay soil profile at larger pile spacings of 6 and 7 m (Fig. 11b). For stiff soil, the increase in raft thickness has minimal effect (compared to soft clay soil profile) on differential settlement reduction, because the stiff soil is sufficiently strong so that thinner raft is also behaved as stiff raft (raft with lower thickness).

3.1.7 Effect of Raft Thickness on Load-Sharing Ratio

The combined effect of t_r and S_p on α_{pr} for PRC2(c) and different soil profiles is shown in Figure 12. It can be seen that with the increase in t_r from 0.5 to 1 m, α_{pr} increases significantly, and when the raft thickness exceeds beyond 1 m, the rate of increase in α_{pr} is observed to be minimal. For any t_r, α_{pr} is higher for the soft clay soil profile compared to that of stiff clay soil profile. Also, it can be noted that at S_p = 7 m, α_{pr} reaches the value equal to 1.

It indicates that the entire applied load has been carried by piles only. In the soft clay soil profile, raft–soil contact pressure is relatively lower than that of stiff clay soil profile. Thus, because of lower raft–soil contact pressure, the maximum capacities of piles are mobilized in soft clay soil profile.

3.1.8 Effect of Raft Thickness on Maximum Bending Moment and Maximum Shear Force

The maximum bending moment and maximum shear force in raft are considerably affected by the raft thickness. Normally, raft of lower thickness is susceptible for larger differential settlement and substantial bending because of its flexibility, whereas comparatively thicker raft may be uneconomical because of the requirement of huge amount of concrete. Figure 13 shows the effect of t_r and S_p on M_{max} and τ_{max} for PRC2(c) and different soil profiles. For any soil profile, M_{max} increases as the t_r increases.

For any soil profile, M_{max} is lower at smaller t_r with S_p = 6 m and higher at greater t_r with S_p = 7 m (Fig. 13a). In comparison with M_{max}, τ_{max} decreases marginally as the t_r increases. It can also be observed that τ_{max} is lower for soft clay profile than that for stiff clay profile. This is due to the lower resistance offered by the soft clay soil profile as compared to the stiff clay soil profile. Thus, the raft

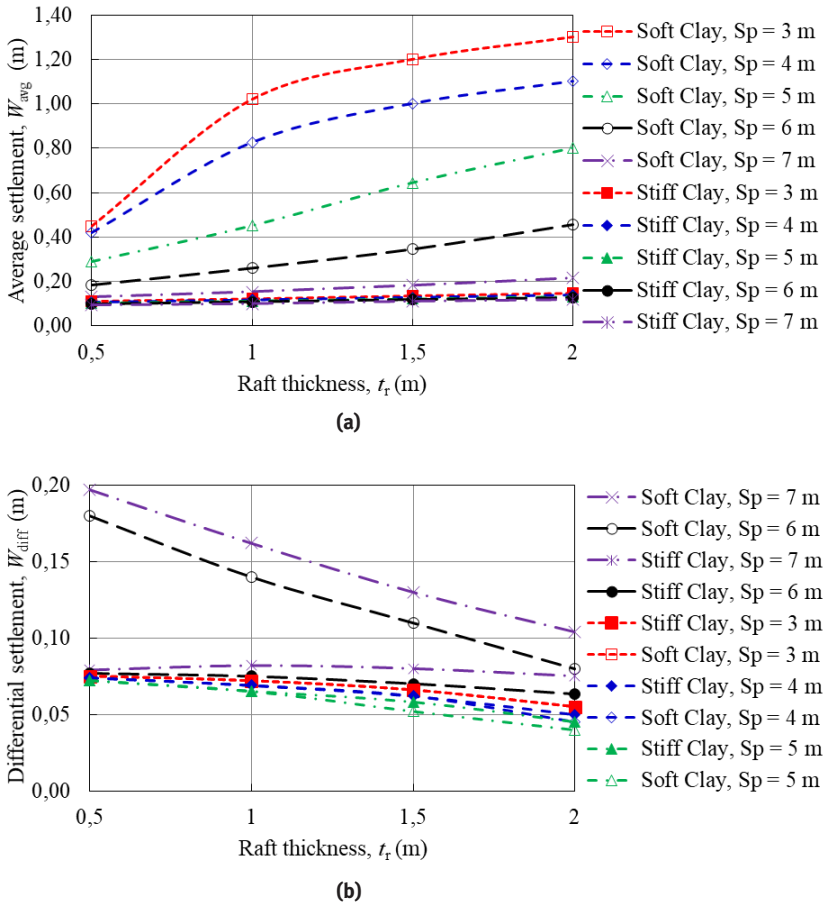

Figure 11: Combined effect of raft thickness and pile spacing on (a) average settlement and (b) differential settlement for PRC2 (c)

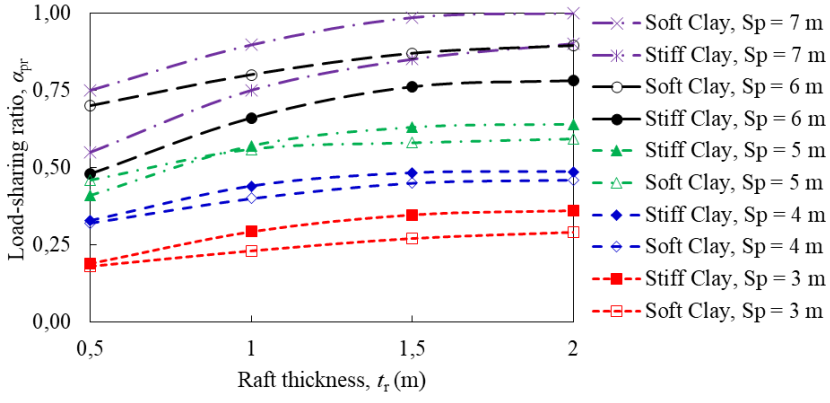

Figure 12: Combined effect of raft thickness and pile spacing on load-sharing coefficient for PRC2(c)

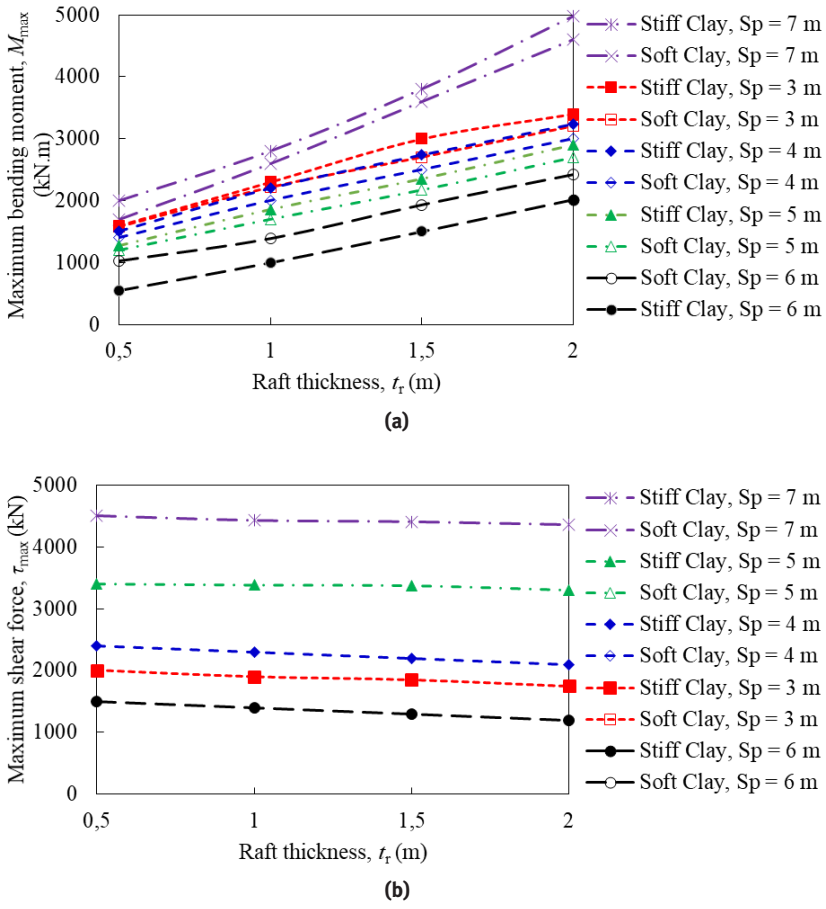

Figure 13: Combined effect of raft thickness and pile spacing on (a) maximum bending moment and (b) maximum shear force for PRC2(c)

thickness should be selected in such way that differential settlement should be within tolerable limit, and bending moment and shear force in the raft should be least so that the economical and efficient design of piled raft can be achieved.

3.1.9 Behavior of Piles in Piled-Raft

In this section, the effect of pile spacing on the pile head settlement, pile axial load (Q_p), and maximum bending moment in piles (M_{maxp}) for center pile (P_1), edge pile (P_{40}), and corner pile (P_{37}) are presented and discussed. The effect of pile spacing on aforementioned behaviors of piles in soft clay soil profile has been considered in this section, and the results are presented. As expected, it can be seen from Figure 14 that center pile (P_1) settle more followed by edge pile (P_{40}) and then the corner pile (P_{37}), which settles lesser. Also, with the increases in S_p, the pile head settlement decreases significantly.

The effect of S_p on axial pile load Q_p for soft clay soil profile is shown in Figure 15(a). It can be seen that with the increase in S_p, the axial load carried by piles increases. Also it can be noted that the length of corner pile (P_{37}) is lesser compared to center pile (P_1); however, corner pile (P_{37}) carries maximum load followed by edge pile (P_{40}) and then center pile (P_1). The corner pile (P_{37}) bends because of lower confinement (relative to edge and center pile), and because of this, the axial load carried by corner pile is more than other piles (Fig. 15b). The effect of S_p on maximum bending moment of piles (M_{maxp}) is shown in Figure 16. Initially, with the increase in S_p from 3 to 4 m, M_{maxp} increases and then decreases as the S_p reaches to 4 m, thereafter M_{maxp} increases gradually. It can be seen that M_{maxp} is higher in corner pile (P_{37}) and lower in center pile (P_1).

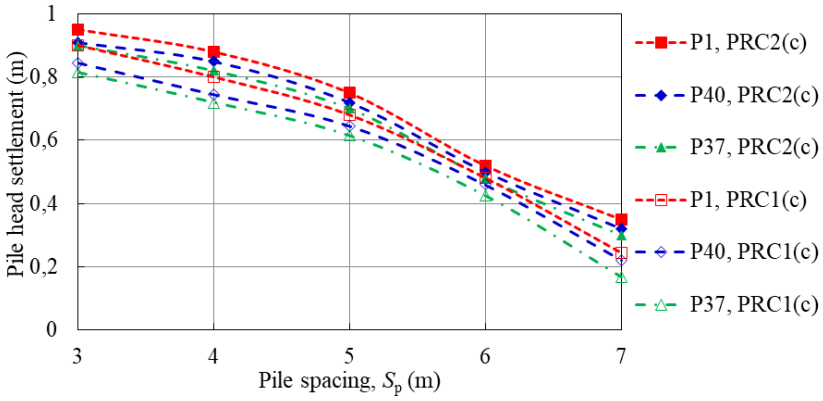

Figure 14: Effect of pile spacing on pile head settlement

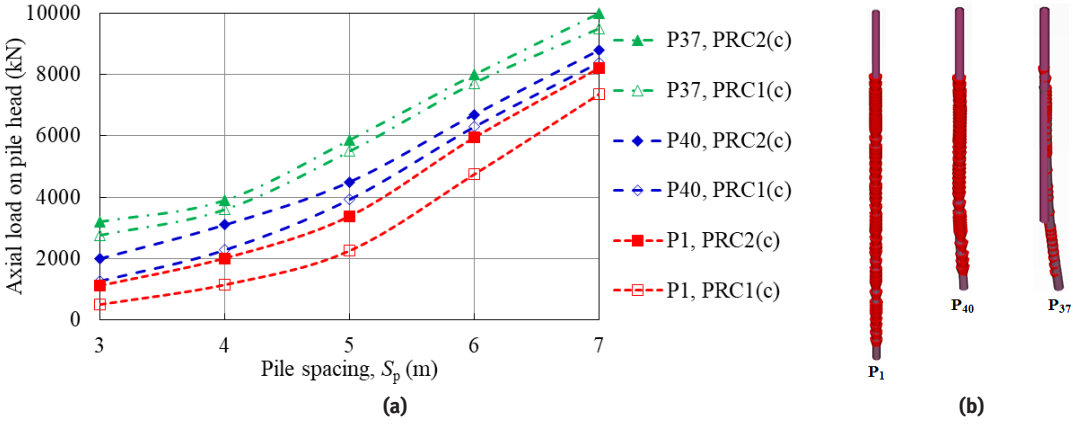

Figure 15: (a) Effect of pile spacing on pile axial load and **(b)** bending in different piles

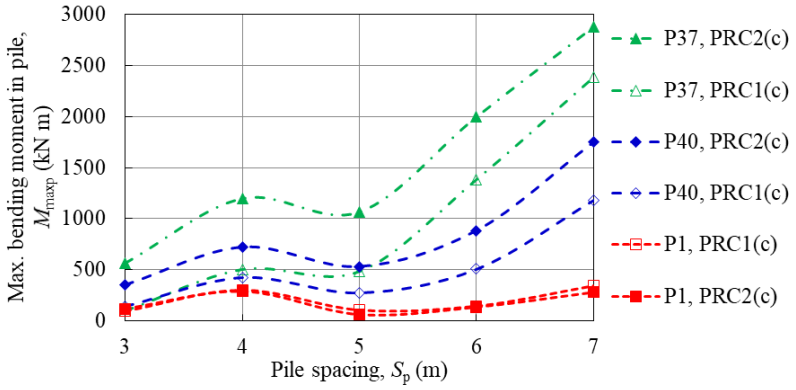

Figure 16: Effect of pile spacing on maximum bending moment in piles

4 Conclusions

In the present study, three-dimentional finite-element model is used to evaluate the settlement, load-sharing, bending moment, and shear force behavior of piled-raft foundation on different soil profiles for different load configurations and PRCs. In order to understand behaviors, the parameters such as pile spacing and raft thickness were varied. The behavior of soil continuum was modeled efficiently by the Mohr–couloumb elastic-plastic model. The PLAXIS 3D software, which is based on solid mechanics principles, was used successfully to simulate the stated problem. The following conclusions can be drawn for PRCs of equal applied load and equal total length of pile (1,470 m):

1. For any soil profile, with the increase in pile spacing, the average settlement decreases and the differential settlement increases; however, in soft clay soil profile, significant decrease in average settlement and substantial increase in differential settlements were observed similar to those of the stiff clay soil profile. Also, with the increase in pile spacing, there is an increase in the load-sahring ratio, maximum bending moment, and maximum shear force (except S_p = 6 m). The maximum bending moment and maximum shear force were lower in soft clay soil profile.
2. For any soil profile, the average settlement, differential settlement, load-sharing coefficient, maximum bending moment M_{max} and maximum shear force τ_{max} are observed to be lower for piled-raft configurations with uniformaly distributed load as compared to the piled-raft configurations with equivalent point load.
3. For soft clay soil and stiff soil profile, "W"-shaped PRC and "V"-shaped PRC with larger pile spacing wer more effective to reduce the average settlement. Furthermore, for any soil profile, the "W"-shaped PRC was most effective in increasing the load-sharing coefficient, whereas the "V"-shaped PRC was more effective in reducing the differentail settlement, bending moment, and maximum shear force.
4. For any soil profile, with the increase in raft thickness, the average settlement increases and the differential settlement decreases; however, in soft clay soil profile, significant increases in average settlement and substantial decreases in differential settlements were observed, similar to those of the stiff clay soil profile. Also, with the increase in raft thickness from 0.5 to 1 m, load-sharing ratio increases significantly and thereafter the effect is marginal. The PRC with lower raft thickness and larger pile spacing was effective in achieving the minimum bending moment and minimum shear force.
5. For soft clay profile, with the increases in pile spacing, the pile head settlement decreases and the axial load Q_p carried by the piles increases. The center pile (P_1) settle more followed by edge pile (P_{40}) and then the corner pile (P_{37}). The axial load Q_p and maximum bending moment M_{maxp} in piles were maximum in corner pile (P_{37}) and decreased for edge pile (P_{40}) and center pile (P_1). In corner and edge piles, the maximum bending moment was observed to be subtantial for equvalent point load similar to that of uniformlay distributed loading.

References

[1] Brinkgreve, R., Swolfs, W., and Engin, E. (2015). PLAXIS user's manual, version 6.1, Balkema, Rotterdam, The Netherlands

[2] Burland, J. B. (1995). "Piles as settlement reducers." *Proce. of 19th National Italian Geotechnical Conference*, *Italy,* Vol 2, 21-34.

[3] Cho, J., Lee, J., Jeong, S., and Lee, J. (2012). "The settlement behavior of piled raft in clay soils." *Ocean Engineering*, 153-163.

[4] Chow, H. S. W., and Small, J. C. (2005). "Behaviour of piled rafts with piles of different lengths and diameters under vertical loading." *Advance in Deep Foundations*, 1-15. DOI: 10.1061/40778(157)20.

[5] Ghalesari A. T., Barari, A. P., and Fardad, A. I. L. B. (2015). "Development of optimum design from static response of pile-raft interaction." *Journal of Material Science and Technology*, 20, 331-343.

[6] Ghalesari, A. T., and Choobbasti, A. J. (2016). "Numerical analysis of settlement and bearing behaviour of piled raft in Babol clay." *European Journal of Environmental and Civil Engineering*, 1-26. DOI: 10.1080/19648189.2016.1229230.

[7] IS 1904-1986 Code of practice for design and construction of foundations in soils. *Bureau of Indian Standards*, New Delhi, India.

[8] Lee. J., Kim. Y., and Jeong. S. (2010). "Three dimentional analysis of bearing behavoir of piled raft on soft clay." *Computers and Geotechnics*, 37, 103-114.

[9] Mali S, Singh B. (2018). "Behavior of large piled-raft foundation on clay soil." *Ocean Engineering*, 149, 205-216.

[10] Mali S, Singh B. (2019). "Behavior of large piled-raft foundation on different soil profiles for different loadings and different piled-raft configurations." *Innovative Infrastructures Solutions*, DOI: 10.1007/s41062-018-0193-9.

[11] Nguyen, D. D. C., Kim, D S., and Jo, S. B. (2013). "Settlement of piled rafts with different pile arrangement schemes via centrifuge tests." *Journal of Geotechnical and Geoenvironmental Engineering*, 139(10), 1690-1698.

[12] Poulos, H. G., and Devdas, A. J. (2005). "Foundation design for the Emirates twin towers Dubai." *Candian Geotechnical Journal*, 42, 716-730.

[13] Poulos, H. G., and Bunce, G. (2008). "Foundation design for the Burj Dubai: The world tallest building." *Proc. of 6th Int. Conf. on Case Histories in Geotechnical Engineering*, Arlinton, VA, 11-16.
[14] Poulos, H. G., Small, J. C., and Chow, H. (2011). "Piled raft foundation for tall buildings." *Geotechnical Engineering Journals of the SEAGS and AGSSEA*, 42(2), 78-84.
[15] Poulos, H. G. (2001). "Methods of analysis of piled raft foundations." *A Report Prepared on Behalf of Technical Committee TC18 on Piled Foundations*.
[16] Prakoso, W. A., and Kulhawy, F. H. (2001). "Contribution to piled raft foundation design." Journal *of Geotechnical and Geoenvironmental Engineering*, 127(1), 17-24.
[17] Rabiei, M., and Choobbasti, A. J. (2016). "Piled raft design strategies for high rise buildings." *Geotechnical Geological Engineering*, 34, 75-85.
[18] Ranjan, G., and Rao, A. S. R. (2007). "Basic and applied soil mechanics." *New Age International*.
[19] Reul, O. (2004). "Numerical study of the bearing behavior of piled rafts." *International Journal of Geomechanics*, 4(2), 59-68.
[20] Reul, O., and Randolph, M. F. (2004). "Design strategies for piled rafts subjected to nonuniform vertical loading." *Journal of Geotechnical and Geoenvironmental Engineering*, 130, 1-13.
[21] Sanctis, L, D., and Mandolini, A. (2006). "Bearing capacity of the piled rafts on soft clays." *Journal of Geotechnical and Geoenvironmental Engineering*, 132, 1600-1610.
[22] Sinha, A., and Hanna A., M. (2016). "3D Numerical model for piled raft foundation." *International Journal of Geomechanics*, doi.org/10.1061/(ASCE)GM.19435622.0000674
[23] Viggiani, C. (2001). "Analysis and design of piled raft foundations." *First Arrigo Croce Lecture*, *Rivista Italiana Di Geotechnica*, 47-75.